

Formation and Magnetic Properties of Metallic Nickel Nano-Particles

N. M. Deraz*

Chemistry Department, College of Science, King Saud University, Riyadh, Kingdom of Saudi Arabia

*E-mail: nmderaz@yahoo.com

Received: 29 March 2012 / Accepted: 24 April 2012 / Published: 1 May 2012

Crystalline metallic nickel nano-particles were synthesized using combustion route with mixture of glycine and ammonium nitrate. Characterization of the as prepared solids carried out by X-ray diffraction (XRD), transmission electron micrograph (TEM) and vibrating sample magnetometer (VSM) techniques. The XRD results revealed that the metallic nickel nano-particles crystallize in the cubic form using equimolar ratio of glycine and ammonium nitrate. The TEM measurements of the as-synthesized powders showed formation of irregular and homogeneous particles. Using mixture of glycine and ammonium nitrate as fuel for preparation of metallic nickel by combustion method is better than urea which led to formation of nano-crystalline nickel oxide only. The magnetization value of the as prepared Ni measured at room temperature is greater than the value observed for commercial Ni powder.

Keywords: Ni; NiO; TEM; crystallite size; magnetization

1. INTRODUCTION

Recently, synthesis of metal nano-particles (NPs) has gained much importance because their physical and chemical properties differ from those of the bulk particles. Nickel is one of the transition metals which show magnetism and intriguing properties and promising applications [1]. Magnetic nano-materials exhibit different applications in various fields such as conducting paints rechargeable batteries, chemical catalysts, optoelectronics, magnetic recording media, ferro-fluids, magnetic resonance imaging contrast enhancement, drug delivery, hydrogen storage, dyes, pigments, magnetic sensors, memory devices and galvano-magnetic materials [2- 9].

Several different routes have been used for the synthesis of Ni-NPs such as vapor phase method, spray pyrolysis, micro-emulsion, polyol process electrochemical reduction, chemical reduction, sol-gel, combustion reaction and thermal decomposition of organo-metallic precursors [10-

14]. Duan et. al. reported the preparation of hierarchical Ni nano-ring and hollow sphere arrays based on ordered through-pore template and electro-deposition [15]. Chain-like Ni architectures assembled by urchin-like hierarchical nano-particles were obtained by a simple hydrothermal reduction process without the use of any templates or surfactants [16]. Wu et al. [17] reported fabrication of Ni-NPs by hydrazine reduction in ethylene glycol. Authors show that the addition of trace of sodium hydroxide followed by heating at 60 °C is necessary to produce pure Ni-NPs. Roy et al. [18] synthesized oxide-coated Ni-NPs with tetragonal crystalline structure by using borohydride reduction method. The effect of the annealing in the as-prepared sample was efficient to ferromagnetic behavior. Wanget al. [19] prepared Ni-NPs with mean size equal to about 31 nm covered by hydroxyethyl carboxymethyl cellulose (HECMC) layer in solution using hydrazine reduction. Zhang et al. [20] synthesized Ni nano-crystals with diameters in the range of 20–60 nm through decomposition of nickel acetylacetonate in oleylamine.

In addition, the combustion route is a rapidly developing research area. This method is much faster, cleaner and economical relative to conventional method. Recently, Deraz reported the synthesis of metallic nickel nano-powders via combustion technique [14]. A major interest at the moment is in the development of combustion route for the preparation of good-quality Ni-powder. Using of a certain amounts and/or mixture of different fuels can be useful and open a new way for preparing nano-materials to control nano-crystal size, shape and distribution size [14].

The present work reports and discusses the results of the effects of different fuels on the structural, morphological and the saturation magnetization of the as prepared Ni nano-particles.

2. EXPERIMENTAL

2.1. Materials

Two samples were prepared by mixing calculated proportions of nickel nitrate with certain amount of urea or mixture of glycine and ammonium nitrate. The mixed precursors were concentrated in a porcelain crucible on a hot plate at 300 °C for 5 minutes. The crystal water was gradually vaporized during heating and when a crucible temperature was reached, a great deal of foams produced and spark appeared at one corner which spread through the mass, yielding a brown voluminous and fluffy product in the container. In our experiments, the amount of nickel nitrate was fixed at one mole for all samples. The first sample was treated with one mole of urea. The second sample was prepared by using mixture of one mole of glycine and one mole of ammonium nitrate. The prepared solid samples were designated as S1 and S2 for the first and second samples, respectively. The chemicals employed in the present work were of analytical grade supplied by Prolabo Company

2.2. Techniques

An X-ray measurement of the prepared solids was carried out using a BRUKER D8 advance diffractometer (Germany). The patterns were run with Cu K α radiation at 40 kV and 40 mA with scanning speed in 2 θ of 2 ° min⁻¹.

The crystallite size of crystalline phases present in the investigated solids was based on X-ray diffraction line broadening and calculated by using Scherrer equation [23].

$$d = \frac{B\lambda}{\beta \cos \theta}$$

where d is the average crystallite size of the phase under investigation, B is the Scherrer constant (0.89), λ is the wave length of X-ray beam used, β is the full-width half maximum (FWHM) of diffraction and θ is the Bragg's angle.

Transmission electron micrographs (TEM) were recorded on JEOL JAX-840A and JEOL JEM-1230 electron micro-analyzer, respectively. The samples were dispersed in ethanol and then treated ultrasonically in order to disperse individual particles over gold grids.

The magnetic properties of the investigated solids were measured at room temperature using a vibrating sample magnetometer (VSM; 9600-1 LDJ, USA) in a maximum applied field of 15 kOe. From the obtained hysteresis loops, the saturation magnetization (M_s), remanence magnetization (M_r) and coercivity (H_c) were determined.

3. RESULTS

3.1. XRD study

The XRD patterns of S1 and S2 samples are shown in Fig.1.

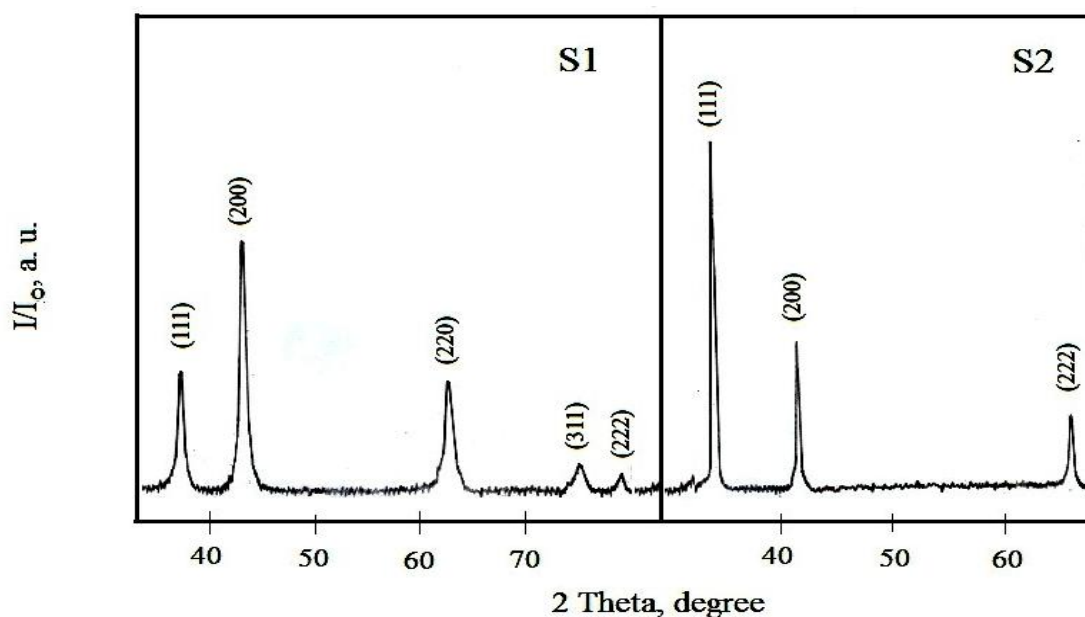


Figure 1. X-ray diffraction patterns of the S1 and S2 samples containing NiO and Ni phases, respectively.

Inspection of These patterns revealed that: (i) The S1 sample consisted of well crystalline NiO crystals. (ii) The S2 sample consisted entirely of well crystalline metallic nickel crystals as a single phase. This finding indicates the promotion effect of the mixture of glycine and ammonium nitrate as fuel in the complete conversion of NiO to produce Ni crystallites. In the XRD patterns, the diffraction lines of Ni and NiO phases are well matched with the reported values in JCPDS files (No. 04-0850 and No. 04.0835, respectively), these phases can be indexed to a cubic structure with the space group $Fm3m$ [14].

From the analysis of XRD data, we can determine the structural parameters such as the crystallite size (d), lattice constant (a) and unit cell volume (V) of crystalline phases. The estimated values of various structural parameters are given in Table 1.

Table 1. Some structural parameters of the as-prepared solids.

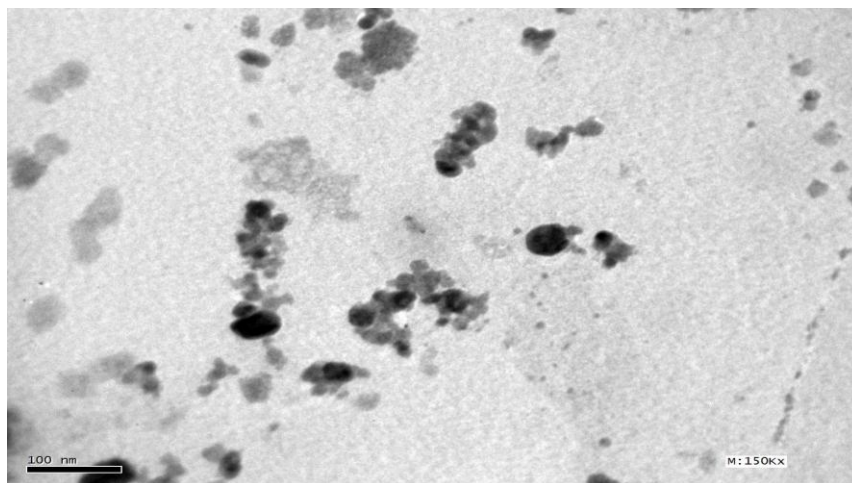
Samples	NiO			Ni		
	d (nm)	a (nm)	V (nm ³)	d (nm)	a (nm)	V (nm ³)
S1	25	4.1802	73.05	-	-	-
S2	-	-	-	80	3.5454	44.56

It can be seen from this table that the mentioned structural parameters for the S2 sample are differed from that for the S1 sample. The observed difference in the values of crystallite size, lattice constant and unit cell volume of the crystalline phases could be attributed to the difference in the flame temperature which assists crystal growth and/or particles adhesion [14]. One can not ignore the difference in nature of solid obtained. In other words, the structural parameters, morphological and magnetic properties of metal nickel are differed from that of nickel oxide. This will discuss later in different sections from this works.

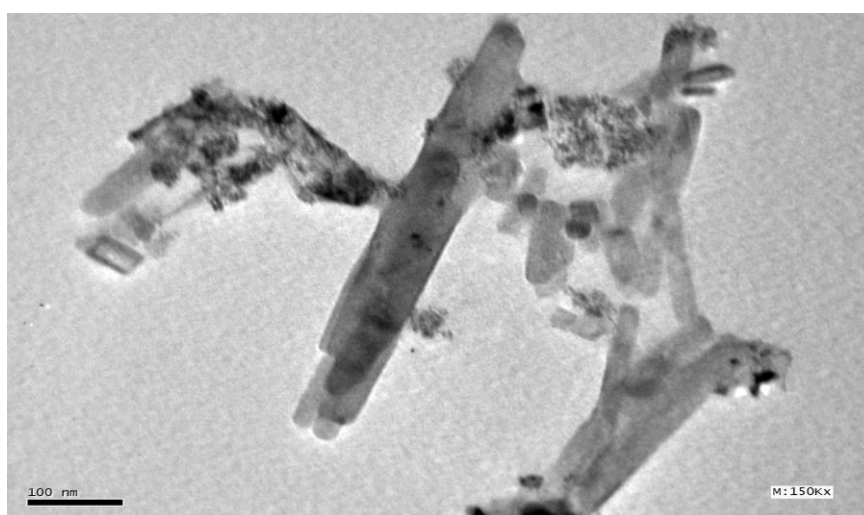
3.2. TEM analysis

Fig. 2a-c shows TEM photographs of S1 and S2 specimens. This figure reveals remarkable changes in microstructure, regarding grain size and partial distribution by adding of fuels to nickel nitrate.

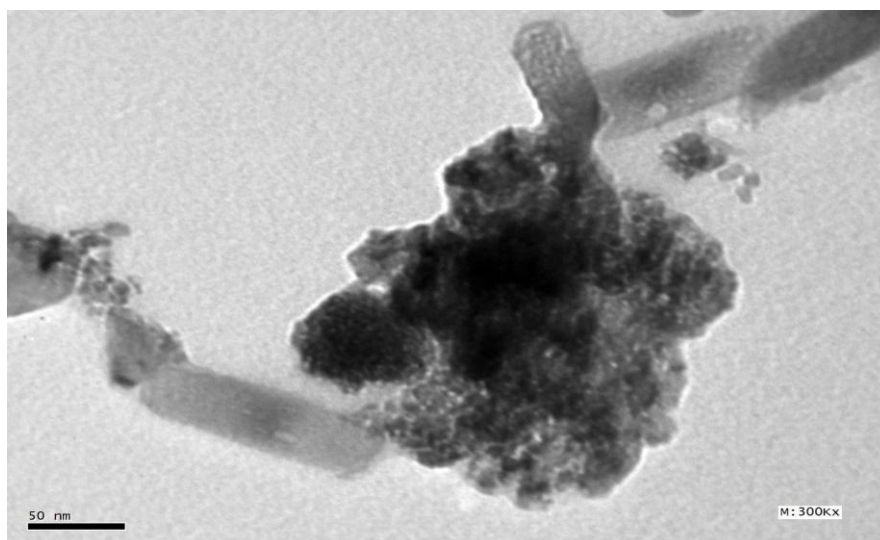
TEM micrograph of the as-prepared powders processed with urea shows slightly tendency to formation of aggregates and/or agglomerates (Fig. 2a). TEM micrograph of the as-prepared powders processed with mixture of glycine and ammonium nitrate shows a relatively heterogeneous grain distribution consisting of bamboo-like tubular nanostructure (Fig. 2b and c). Moreover, there is homogeneous and uniform distribution of these particles in the S2 sample. The agglomeration of the as synthesized particles could be attributed to the local sintering behavior during preparation of the samples by combustion method [14].



A



B



C

Figure 2. TEM images for the as prepared solids: (a) the S1 sample and (b and c) the S2 sample with different magnifications.

3.3. Magnetic properties

The magnetic properties of the as-prepared powders were studied using VSM method. The magnetization behaviors of Ni and NiO are shown in Fig. 3.

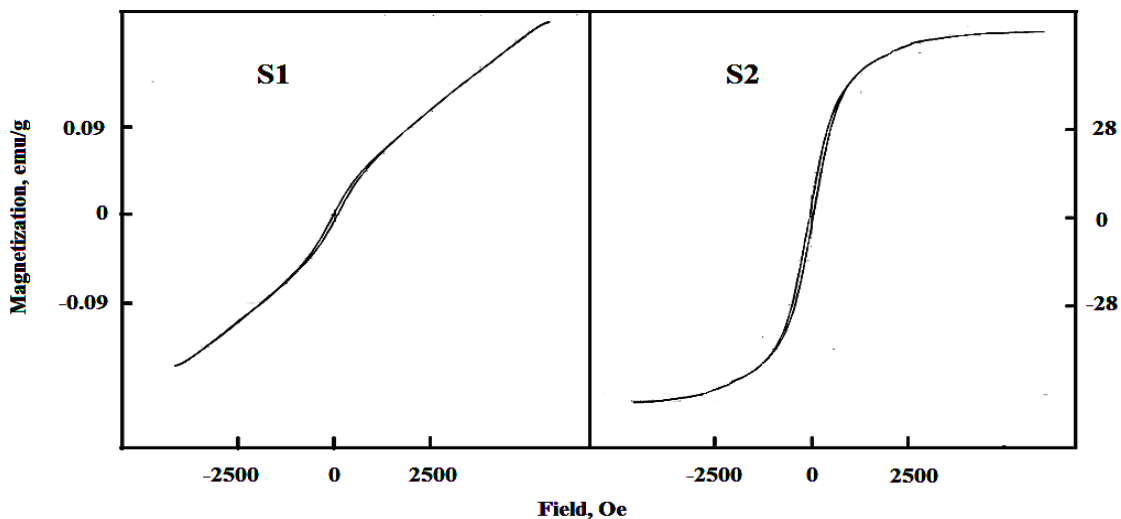


Figure 3. Magnetic hysteresis curves measured at a room temperature for the S1 and S2 samples.

The magnetic field versus magnetization curve at room temperature is recorded with the field strength of -15 kOe to 15 kOe. From these measurements, the saturation magnetization (M_s), remanence magnetization (M_r) and coercivity (H_c) are derived and listed in Table 2.

Table 2. The magnetic properties (M_s , M_r and H_c) of the as-prepared solids.

Samples	M_s (emu/g)	M_r (emu/g)	M_r/M_s (emu/g)	H_c (Oe)
S1	00.198	0.02	0.093	60.85
S2	60.000	10.93	0.182	68.11

It can be seen that there is no saturation magnetization observed for the S1 sample up to the field strength of 15kOe. On the other hand, the saturation magnetization for the S2 sample was found to be 60 emu/g. It was found that the S2 sample containing exhibited a saturation magnetization greater than that of the bulk nickel (55 emu/g) [21]. In one of my previous work, it was found that nickel metal can be prepared by combustion method using 1.5 mol glycine with saturation magnetization of 57.39 emu/g [14]. Also, the mentioned work indicates that 1 mole glycine is not sufficient for preparing

metallic nickel only but led to prepare mixture of Ni and NiO with saturation magnetization of 57.04 emu/g [14].

4. DISCUSSION

The literature survey reported that the characteristics of the product of preparation process depend largely on the crystallite size and particle distribution, synthesis route and experimental conditions, e.g. NiO can be pale apple green or jet black depending up on the stoichiometry. In addition, the insulator NiO can be green while the black material behaves like a p-type semiconductor due to deficiency of Ni²⁺ ions [22]. However, the ratio between the glycine as fuel and nickel nitrate affect the formation of single or mixture of Ni and NiO phases in the Ni/NiO system [14].

In this work, the combustion route resulted in formation of single phase of NiO using urea as fuel and formation nano- crystalline metallic nickel using mixture of glycine and ammonium nitrate. Indeed, well crystalline NiO and Ni phases were detected in the X-ray diffraction patterns using urea and mixture of glycine and ammonium nitrate, respectively. This indicates the role of mixture of glycine and ammonium nitrate as fuels in the promotion of the metallic nickel formation.

During the chemical reaction for the preparation of the proposed materials via the combustion route, the different physical and chemical processes expected to occur in an instantaneous moment are given in four steps [23] as follows: (i) the first step is the decomposition of the fuel. (ii) The next step is the decomposition of the reactants into their respective oxides with the liberation of nitrate ions and water. (iii) The nitrate ions combine with the ammonium ion to form ammonium nitrate. The ammonium nitrate so formed is responsible for fuelling the combustion process. Initiation of the combustion occurs when ammonium nitrate is uniformly distributed in the region of reaction. In addition, the promotion of combustion process maybe increases when we use mixture of ammonium nitrate with the fuel used during the preparation process. The released heat due to the above three stages is sufficient for the formation and subsequent crystallization of the desired product.

The released heat, during the combustion process, helps in crystallization and formation of the desired phase such as well crystalline NiO and Ni nano- particles involved in this work. This heat resulted in significant effects on different properties of the products such as the crystallite size, homogeneity, particle distribution, porosity, surface area and the sintering process. One of advantages of the combustion method liberates of gaseous products which dissipates the heat of combustion and limits the rise of temperature. This advantage resulted in reduce the possibility of local partial sintering among the primary particles [14]. In fact, the gases evolved during the combustion reaction brought about formation of nano- sized Ni and NiO with less agglomeration as shown in Fig. 2a-c.

In this study, the different fuels yielded much changes in structural and morphological characteristics of the as- prepared solids powders which subsequent significant modifications in their magnetic properties [14, 24]. Non-saturating behavior of some materials indicates the presence of two components: (i) ferro/ferrimagnetic and (ii) superparamagnetic or paramagnetic [25]. Very low magnetization value of the S1 sample could be attributed to the observed superparamagnetism and weak ferromagnetism in nickel oxide as well as the contribution towards the magnetic moment arising

from other sources such as the presence of non-stoichiometry and/or Ni³⁺ ions [14, 26]. This behavior is the characteristic property of antiferromagnets. High magnetization value of the S2 sample could be understood as a result of the finite-size and surface effects [14, 27]. Finally, the magnetization critically depends on the microstructure of the interface (roughness and crystallinity degree) that determines the spin configuration [28].

5. CONCLUSIONS

Nano-crystalline NiO powder can be prepared using a simple urea assisted combustion technique. Mixture of equimolar ratio of glycine and ammonium nitrate led to well crystalline metallic nickel. The crystallite size, lattice constant and unit cell volume of Ni are differed from that of NiO nano- particles. The shape, grain size and the homogeneity of the as prepared solids are dependent on the nature of fuel. The magnetization value of Ni measured at room temperature is greater than that observed for commercial Ni powder and also the metallic nickel prepared by glycine only in previous my work [14].

ACKNOWLEDGEMENT

The project was supported by the Research Center, College of Science, King Saud University.

References

1. A. Alarifi, N. M. Deraz, S. Shaban, *J. Alloy Comps* 486 (2009) 501.
2. S. Hironari, Y. Nakano, H. Matsushita, A. Onoe, H. Kanai, Y. Yamashita, *J. Mater. Synth. Process.* 6 (1998) 415.
3. E. Antolini, M. Ferretti, S. Gemme, *J. Mater. Sci.* 31 (1996) 2187.
4. L.N. Lewis, *Chem. Rev.* 93 (1993) 2693.
5. L.L. Beecroft, C.K. Ober, *Chem. Mater.* 9 (1997) 1302.
6. S. Morup, in: A. Hernando (Ed.), *Studies of Superparamagnetism in Samples of Ultrafine Particles, Nanomagnetism*, Kluwer Academic Publishers, Boston, 1993, pp. 93.
7. A. Aharoni, *Introduction to the Theory of Ferromagnetism*, Oxford University Press, New York, 1996, pp. 133.
8. U. Hafeli, W. Schutt, J. Teller, M. Zborowski (Eds.), *Scientific and Clinical Applications of Magnetic Carriers*, Plenum Press, New York, 1997.
9. I. Safarik, M. Safarikova, *Monatsh. Chem.* 133 (2002) 737.
10. Y. Hou, H. Kondoh, T. Ohta, S. Gao, *Appl. Surf. Sci.* 241 (2005) 218.
11. N. Cordente, C. Amiens, B. Chaudret, M. Respaud, F. Senocq, M.J. Casanove, *J. Appl. Phys.* 94 (2003) 6358.
12. J. Gong, L.L. Wang, Y. Liu, J.H. Yang, Z.G. Zong, *J. Alloys Compd.* 457 (2008) 6.
13. N. M. Deraz, M.M. Selim, M. Ramadan, *Mater. Chem. Phys.* 113 (2009) 269.
14. N. M. Deraz, *Current Applied Physics* 12 (2012) 928.
15. G.T. Duan, W.P. Cai, Y.Y. Luo, Z.G. Li, Y. Lei, *J. Phys. Chem. B* 110 (2006) 15729.
16. L.P. Zhu, G.H. Liao, W.D. Zhang, Y. Yang, L.L. Wang, H.Y. Xie, *Eur. J. Inorg. Chem.* (2010) 1283.

17. S.H. Wu, D.H. Chen, *J. Colloid Interface Sci.* 259 (2003) 282.
18. A. Roy, V. Srinivas, S. Ram, J.A. De Toro, U. Mizutani, *Phys. Rev. B* 71 (2005) 184443.
19. H. Wang, X. Kou, J. Zhang, J. Li, *Bull. Mater. Sci.* 31 (2008) 97.
20. H.T. Zhang, G.Wu, X.H. Chen, X.G. Qiu, *Mater. Res. Bull.* 41 (2006) 495.
21. J.H. Hwang, V.P. Dravid, M.H. Teng, J.J. Host, B.R. Euiott, D.L. Johnson, T.O. Mason, *J. Mater. Res.* 12(1997) 1076.
22. W. J. Moore, in: R. Johnsen (Ed.), *Seven Solid States: An Introduction to the Chemistry and Physics of Solids*, WA Benjamin, INC, New York, 1967, pp. 133.
23. P. Priyadharsini, A. Pradeep, G. Chandrasekaran, *J. Magn Magn. Mater.* 321(2009)1898.
24. Z. Liu, S. Li, Y. Yang, S. Peng, Z. Hu, Y. Qian, *Adv. Mater.* 15(2003)1946.
25. Rucha Desai, R.V. Mehta, R.V. Upadhyay, Amita Gupta, A. Praneet, K.V. Rao, *Bull. Mater. Sci.* 30 (2007) 197.
26. T. Richardson, D.I. Yiagas, B. Turk, K. Forster, M.A. Twigg, *J. Appl. Phys.* 70 (1991) 6977.
27. R.D. Zysler, H. Romero, C.A. Ramos, E. De Biasi, D. Fiorani, *J. Magn. Magn. Mater.* 266 (2003) 233.
28. J. Noguees, I.K. Schuller, *J. Magn. Magn. Mater.* 192 (1999) 203.